Dosimetry of 64Cu-DOTA-AE105, a PET tracer for uPAR imaging

Persson, Morten; El Ali, Henrik H.; Binderup, Tina; Pfeifer, Andreas Klaus; Madsen, Jacob; Rasmussen, Palle; Kjær, Andreas

Published in:
Nuclear Medicine and Biology

Link to article, DOI:
10.1016/j.nucmedbio.2013.12.007

Publication date:
2014

Document Version
Publisher's PDF, also known as Version of record

Nuclear Medicine and Biology 41 (2014) 290–295

Contents lists available at ScienceDirect

Nuclear Medicine and Biology

journal homepage: www.elsevier.com/locate/nucmedbio

Dosimetry of ^{64}Cu-DOTA-AE105, a PET tracer for uPAR imaging

Morten Persson [a,b,c], Henrik H. El Ali [b,c], Tina Binderup [b,c], Andreas Pfeifer [b,c], Jacob Madsen [b], Palle Rasmussen [d], Andreas Kjaer [a,b,c,*]

[a] The Danish-Chinese Center for Proteases and Cancer
[b] Department of Clinical Physiology, Nuclear Medicine & PET, Center for Diagnostic Investigations, Rigshospitalet, Copenhagen, Denmark
[c] Cluster for Molecular Imaging, Faculty of Health Sciences, University of Copenhagen, Copenhagen, Denmark
[d] Hevesy Laboratory, DTU Nutech, Technical University of Denmark, Kongens Lyngby, Denmark

ARTICLE INFO

Article history:
Received 20 September 2013
Received in revised form 28 November 2013
Accepted 7 December 2013

Keywords:
uPAR
Urokinase
Dosimetry
PET
DOTA
Peptide
Translational

ABSTRACT

^{64}Cu-DOTA-AE105 is a novel positron emission tomography (PET) tracer specific to the human urokinase-type plasminogen activator receptor (uPAR). In preparation of using this tracer in humans, as a new promising method to distinguish between indolent and aggressive cancers, we have performed PET studies in mice to evaluate the *in vivo* biodistribution and estimate human dosimetry of ^{64}Cu-DOTA-AE105.

Methods: Five mice received iv tail injection of ^{64}Cu-DOTA-AE105 and were PET/CT scanned 1, 4.5 and 22 h post injection. Volume-of-interest (VOI) were manually drawn on the following organs: heart, lung, liver, kidney, spleen, intestine, muscle, bone and bladder. The activity concentrations in the mentioned organs [%ID/g] were used for the dosimetry calculation. The %ID/g of each organ at 1, 4.5 and 22 h was scaled to human value based on a difference between organ and body weights. The scaled values were then exported to OLINDA software for computation of the human absorbed doses. The residence times as well as effective dose equivalent for male and female could be obtained for each organ. To validate this approach, of human projection using mouse data, five mice received iv tail injection of another ^{64}Cu-DOTA peptide-based tracer, ^{64}Cu-DOTA-TATE, and underwent same procedure as just described. The human dosimetry estimates were then compared with observed human dosimetry estimate recently found in a first-in-man study using ^{64}Cu-DOTA-TATE.

Results: Human estimates of ^{64}Cu-DOTA-AE105 revealed the heart wall to receive the highest dose (0.0918 mSv/MBq) followed by the liver (0.0815 mSv/MBq), All other organs/tissue were estimated to receive doses in the range of 0.02–0.04 mSv/MBq. The mean effective whole-body dose of ^{64}Cu-DOTA-AE105 was estimated to be 0.0317 mSv/MBq. Relatively good correlation between human predicted and observed dosimetry estimates for ^{64}Cu-DOTA-TATE was found. Importantly, the effective whole body dose was predicted with very high precision (predicted value: 0.0252 mSv/Mbq, Observed value: 0.0315 mSv/MBq) thus validating our approach for human dosimetry estimation.

Conclusion: Favorable dosimetry estimates together with previously reported uPAR PET data fully support human testing of ^{64}Cu-DOTA-AE105.

1. Introduction

The serine protease urokinase-type plasminogen activator (uPA) and its receptor (uPAR) have been shown to be up-regulated during cancer invasion and metastatic development [1–4]. By localized proteolytic activity, causing degradation of the extracellular matrix, uPAR facilitates cancer cells to escape the primary tumor and to be transported by the vascular and/or lymphatic system to distal sites where new metastatic lesions are established. In line with this, multiple studies have, based on immunohistochemistry on biopsies and blood-based ELISA, reported uPAR to be a strong prognostic marker for poor prognosis and metastatic disease in a number of cancers, including breast, prostate, colorectal, gastric and lung cancer [3–11]. This makes uPAR a very interesting target for non-invasive PET imaging, since this could enable a whole-body quantitative analysis of uPAR expression in both the primary tumor and metastatic lesions [12–14]. The development of a uPAR PET tracer could circumvent the well-known limitations using random biopsies and/or blood samples as an in-direct method for uPAR expression in the tumor tissue, and hopefully provide improved diagnostic and prognostic information for the individual patient.

Based on the small linear peptide AE105 with high affinity for uPAR, ^{64}Cu-DOTA-AE105 is one of several promising uPAR PET tracers recently developed in our group [15–19]. Before considering translation into human use, estimates of human dosimetry are important. To date, there have been only a limited number of studies that have compared and validated mouse-derived predicted

* Corresponding author at: Department of Clinical Physiology, Nuclear Medicine & PET Copenhagen University Hospital – 4012 Blegdamsvej 9 2100 – Copenhagen Ø Denmark.
E-mail address: akjaer@sund.ku.dk (A. Kjaer).

0969-8051/$ – see front matter © 2014 Elsevier Inc. All rights reserved.
http://dx.doi.org/10.1016/j.nucmedbio.2013.12.007

dosimetry of PET radiotracers with human observed dosimetry data [20–25]. All these studies have used conventional biodistribution analysis of dissected mouse tissue at different time points to estimate human dosimetry. Despite the obvious differences in anatomy and physiology between mice and man, relatively close correlation between predicted vs. observed dosimetry have however been found, exemplified by close predictions of 4 out of 6 PET tracers in the study by Sakata and co-workers [22]. Moreover, recently two studies have reported the use of PET image-derived biodistribution analysis in mice for use to estimate human dosimetry [26,27]. Importantly, a significant correlation between conventional biodistribution tissue analysis and image-derived analysis were reported ($p = 0.9666$), thus validating this new approach [27].

Therefore, in the present study we evaluated the *in vivo* biodistribution of ^{64}Cu-DOTA-AE105 in mouse organs using whole-body microPET/CT imaging. Residence times were estimated using the radiation dose assessment resource (RADAR) models and were extrapolated to humans based on simple assumptions on difference between the species using the OLINDA dosimetry software. To verify that human projection based on image-derived mouse biodistribution data from three time-points is a reasonable approach, we performed a correlation analysis between projected human dosimetry based on mouse data from whole body microPET/CT for the somatostatin receptor-targeting PET tracer ^{64}Cu-DOTA-TATE with data from a recently human ^{64}Cu-DOTA-TATE dosimetry PET study in our group [28]. This article therefore present the first human dose estimates for ^{64}Cu-DOTA-AE105 based on mice studies and validates the approach using ^{64}Cu-DOTA-TATE as an example.

2. Materials and methods

2.1. Tracer synthesis

^{64}Cu was produced on a PETtrace cyclotron (GE Healthcare) equipped with a beamline. The production of ^{64}Cu was carried out via the ^{64}Ni(p,n)^{64}Cu nuclear reaction using a solid target system consisting of a water cooled target mounted on the beamline. The target consisted of ^{64}Ni metal (enriched to >99%) electroplated on a silver disc backing. A proton beam of 16 MeV and a beam current of 20 μA were used. After irradiation, the target was transferred to the laboratory for further chemical processing where ^{64}Cu was isolated using ion exchange chromatography. Final evaporation from aqueous HCl yielded 2–6 GBq ^{64}Cu as $^{64}CuCl_2$.

^{64}Cu-DOTA-AE015 were synthesized by adding $^{64}CuCl_2$ (≈150 MBq) to a vial containing 0.1 M ammonium acetate buffer (pH = 8) and peptide (2 nmol), with a temperature of 70 °C. The labeling of DOTA-AE105 took 60 min and resulted in greater than 95% yield. No additional radiochemical purification step was required. The amount of unlabeled ^{64}Cu in the product was less than 1%, as demonstrated by radio-TLC. The specific activity was approximately 40 MBq/nmol.

DOTA-TATE was radiolabeled as recently described [28]. In brief, DOTA-TATE was labeled with ^{64}Cu by adding a sterile solution of DOTA-TATE (0.3 mg) and gentisic acid (25 mg) in aqueous sodium acetate (1 mL; 0.4 M, pH 5.0) to a dry vial containing $^{64}CuCl_2$ (800–1000 MBq) at ambient temperature for 10 min and diluted with 1 mL water. Finally, the mixture was passed through a Millex-GP 0.22-mm sterile filter (Millipore). The amount of unlabeled ^{64}Cu in the product was less than 1%, as demonstrated by radio-TLC. The specific activity was approximately 5 MBq/mmol.

2.2. Animal

A total of 10 mice (NMRI Nude, Taconic) were used in this study. The animals were housed in 2 cages with 5 animals in each in a climate-controlled room with 12:12-h light cycle. Animals had free access to food and water during housing.

2.3. MicroPET/CT

Five mice received tail vein injection of ^{64}Cu-DOTA-AE105 (6 MBq) and five mice received ^{64}Cu-DOTA-TATE (6 MBq). PET scans were acquired with a microPET Focus 120 scanner (Siemens Medical Solutions, Malvern, PA). The energy window of the emission scans was set to 350–605 keV with a time resolution of 6 ns. The acquired emission dataset was automatically stored in listmode. Each mouse was PET/CT scanned 1, 4.5 and 22 h post injection: 10 min static PET scan followed by a CT scan. CT data were acquired with a MicroCAT II tomograph (Siemens Medical Solutions, Malvern, PA). The x-ray tube with a 0.5-mm aluminum filter was set at a 80 kVp, a tube current of 500 μA, and an exposure time of 700 ms per projection. The voxel size was 0.095 × 0.095 × 0.095 m m^3. During the scanning, the animal was anesthetized using 2% isoflurane.

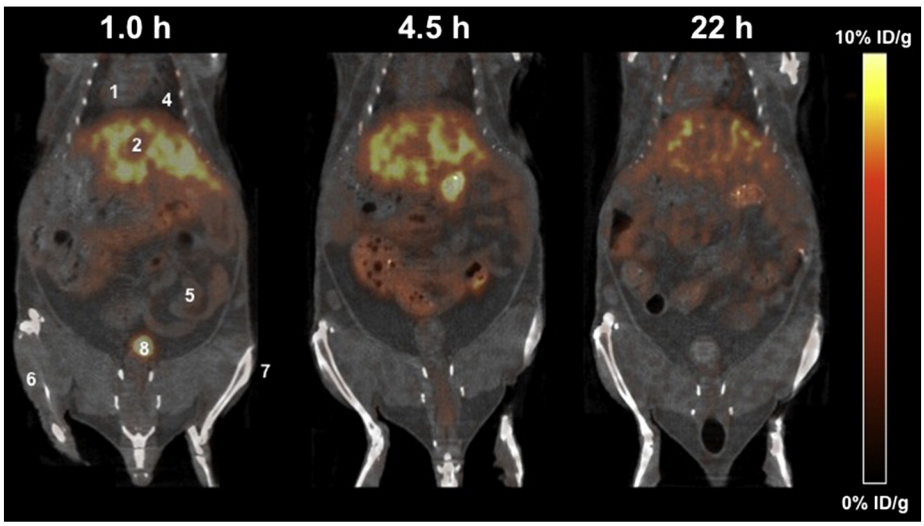

Fig. 1. Representative PET/CT images 1, 4.5 and 22 h post intravenous injection of ^{64}Cu-DOTA-AE105 in the tail vein (6 MBq/0.24 μg peptide). Numbers in the picture indicates location of organs used for ROI analysis: 1) Heart/Blood, 2) Liver, 3) Kidney (not shown in this image), 4) Lung, 5) Intestine, 6) Muscle, 7) Bone, 8) Bladder.

Table 1
Mouse biodistribution of 64Cu-DOTA-AE105.

Source Organ	1 h	4.5 h	22 h
Blod	1.3 ± 0.5	1.5 ± 0.5	1.4 ± 0.6
Liver	12.3 ± 5.0	9.6 ± 4.6	6.2 ± 2.5
Kidney	3.9 ± 2.4	3.2 ± 1.3	2.9 ± 1.2
Lung	1.3 ± 0.4	1.7 ± 0.63	1.4 ± 0.3
Spleen	5.4 ± 2.0	3.3 ± 1.3	2.6 ± 0.8
Intestine	7.9 ± 2.8	8.6 ± 4.0	2.2 ± 0.7
Muscle	1.0 ± 0.7	0.9 ± 0.6	0.6 ± 02
Bone	0.9 ± 0.4	1.1 ± 0.4	1.1 ± 0.3
Bladder	62.0 ± 53.4	1.9 ± 1.3	0.7 ± 0.6

2.4. Image analysis

All listmode data were postprocessed into 128 × 128 × 32 sinograms using a maximum a priori (3D-MAP) algorithms into 256 × 256 × 95 matrices with a voxel size of 0.43 mm^3. The resolution of the PET scanner was 1.5 mm at CFOV, and 1.8 mm at 38 mm off-centre using 3D-MAP. All results were analyzed using Inveon software (Siemens Medical Solutions, Malvern, PA, USA) and expressed as percent of injected dose per gram tissue (%ID/g). The mouse organs were identified and 3D volumes of interest were manually drawn on the CT images for all three time-points. The following organs were included in the analysis: blood (heart), liver, kidney, lung, spleen, intestine, muscle, bone and bladder.

2.5. Radiation dosimetry

The projected human doses were then computed for male and females phantoms using OLINDA software (OLINDA/EXM by Vanderbilt University, USA. Version: 1.1) with the human residence times as input. The animal-human biokinetic extrapolation used in this study is the percent kg/g method [29]. The radioactivity concentration in the animal organ data was reported as percent of injected activity per gram of tissue (%ID/g) before using in the below equation for the extrapolation-to-humans:

$$\left(\frac{\%ID}{organ}\right)_{human} = \left[\left(\frac{\%ID}{g}\right)_{animal} \times \left(kg_{TBweight}\right)_{animal} \times \frac{g_{organ}}{\left(kg_{TBweight}\right)_{human}}\right]$$

The animal whole body weight was 34 g (0.034 kg) and the weight of the human organs were chosen from male (73 kg) and female (58 kg) phantoms in OLINDA [30] which was used for the human dosimetry calculation. The urinary elimination fraction was set at 75% within 5 hours. The rest of the activity (25%) assumed to be retained in the body and the removal of the remaining radioactivity can be assumed by only radioactive decay. The extrapolated three point data of the organs i.e. at 1, 4.5, 22 h were used to fit the time activity curve and determine the cumulated activity and residence times.

Table 2
Mouse residence times (Bq × Hr/Bq administrated) of 64CuIDOTAIAE105 in mouse organs.

Source Organ	Mean
Small intestine	1.29E + 00
Heart content	3.83EI01
Kidneys	2.34EI02
Liver	3.85E + 00
Lungs	4.07EI02
Muscle	2.73E + 00
Bone	4.01EI01
Spleen	7.49EI02
Urinary bladder	1.24EI01
Remainder body	6.41E + 00

Table 3
Human residence times (Bq × hr/Bq administrated) estimates of 64Cu-DOTA-AE105 based on mouse residence times and modeled organ mass differences between the two species.

Source Organ	Female	Male
Small intestine	3.00E-01	2.61E-01
Heart content	6.01E-01	5.99E-01
Kidneys	9.11E-02	7.65E-02
Liver	1.17E + 00	1.23E + 00
Lungs	1.24E-01	1.19E-01
Muscle	1.31E + 00	1.66E + 00
Bone	3.00E-01	2.57E-01
Spleen	4.94E-02	4.69E-02
Urinary bladder	3.35E-02	3.43E-02
Reminder body	1.37E + 01	1.34E + 01

2.6. Human ^{64}Cu-DOTA-TATE PET and dosimetry study

Observed human dosimetry data for correlation analysis were taken from a recently published first-in-man ^{64}Cu-DOTA-TATE PET study using data from 5 patients [28].

3. Results

Fig. 1 shows a representative whole-body mouse PET/CT images used for ROI-based distribution analysis of ^{64}Cu-DOTA-AE105 1, 4.5 and 22 h post injection. At 1 h p.i. the bladder and liver presented the highest activity, followed by three organs with similar activity levels, kidney, spleen and intestine. At 4.5 and 22 h, the liver was the organ with highest activity, followed by the intestine. All other organs/tissue had minimal activity levels 4.5 and 22 h p.i (Table 1). Calculated residence-time of ^{64}Cu-DOTA-AE105 derived from VOI analysis and the corresponding human estimated residence times, are shown in Tables 2 and 3, respectively.

The predicted human dosimetry for ^{64}Cu-DOTA-AE105 is shown in Table 4. The heart wall was projected to receive the highest dose in both female and male, respectively (Female: 0.0918 mSv/MBq, Male: 0.0786 mSv/MBq) followed by the liver, osteogenic cells and the small intestine. All other organs/tissue were estimated to receive doses in the range of 0.02-0.04 mSv/MBq. The mean effective whole-body

Table 4
Predicted human dosimetry for 64Cu-DOTA-AE105 (mSv/MBq).

Source Organ	Female	Male
Adrenals	3.31E-02	2.59E-02
Brain	2.84E-02	2.27E-02
Breast	2.69E-02	2.11E-02
Gallbladder wall	3.45E-02	2.83E-02
Lower large intestine wall	3.24E-02	2.50E-02
Small intestine	6.07E-02	4.92E-02
Stomach wall	3.19E-02	2.52E-02
Upper large intestine wall	3.43E-02	2.69E-02
Heart wall	9.18E-02	7.86E-02
Kidneys	3.76E-02	2.97E-02
Liver	8.15E-02	6.38E-02
Lungs	2.32E-02	1.81E-02
Muscle	1.60E-02	1.28E-02
Overies	3.23E-02	2.56E-02
Pancreas	3.39E-02	2.68E-02
Red marrow	2.98E-02	2.41E-02
Osteogenic cells	7.59E-02	5.48E-02
Skin	2.43E-02	1.89E-02
Spleen	3.67E-02	2.88E-02
Testes		2.14E-02
Thymus	3.10E-02	2.41E-02
Thyroid	2.74E-02	2.21E-02
Urinary bladder wall	3.37E-02	2.93E-02
Uterus	3.19E-02	
Total body	3.30E-02	2.58E-02
Effective dose	3.17E-02	2.51E-02

Table 5
Predicted and observed human dosimetry for 64Cu-DOTA-TATE (mSv/MBq).

Source organ	Female predicted	Male predicted*	Male Observed**	Ratio
Adrenals	3.53E-02	2.75E-02	1.37E-01	4.98
Brain	3.36E-02	2.70E-02	1.27E-02	0.47
Breast	3.05E-02	2.40E-02	1.32E-02	0.55
Gallbladder wall	3.52E-02	2.89E-02	3.96E-02	1.37
Lower large intestine wall	3.70E-02	2.86E-02	4.32E-02	1.51
Small intestine	4.40E-02	3.74E-02	6.55E-02	1.75
Stomach wall	3.56E-02	2.83E-02	1.93E-02	0.68
Upper large intestine wall	3.71E-02	2.93E-02	2.18E-02	0.74
Heart wall	6.19E-02	5.10E-02	1.86E-02	0.36
Kidneys	2.08E-02	1.66E-02	1.39E-01	8.37
Liver	4.09E-02	3.19E-02	1.61E-01	5.05
Lungs	1.51E-02	1.19E-02	1.67E-02	1.40
Muscle	1.28E-02	1.04E-02	1.90E-02	1.83
Overies	3.61E-02			
Pancreas	3.66E-02	2.91E-02	9.27E-02	3.19
Red marrow	2.96E-02	2.40E-02	2.65E-02	1.10
Osteogenic cells	7.64E-02	5.64E-02	3.35E-02	0.59
Skin	2.81E-02	2.20E-02	1.22E-02	0.55
Spleen	3.47E-02	2.74E-02	1.15E-01	4.20
Testes		2.51E-02	1.36E-02	0.54
Thymus	3.38E-02	2.60E-02	1.49E-02	0.57
Thyroid	3.17E-02	2.56E-02	1.41E-02	0.55
Urinary bladder wall	5.15E-02	4.35E-02	3.70E-02	0.85
Uterus	3.60E-02			
Total body	3.41E-02	2.64E-02	2.50E-02	0.95
Effective dose	3.17E-02	2.52E-02	3.15E-02	1.25

* Numbers used for correlation analysis in Fig. 2.
** Numbers reproduced from Ref. [28].

dose was estimated to be 0.0317 mSv/MBq (female) and 0.0251 mSv/MBq (male) corresponding to an effective dose of 6.34 mSv and 5.02 mSv, in female and male respectively, after injection of 200 MBq ^{64}Cu-DOTA-AE105 as planned in future clinical trial.

To validate this approach, of human projections from mouse data, a group of mice were injected with another ^{64}Cu-DOTA peptide-based PET ligand, the somatostatin receptor PET ligand ^{64}Cu-DOTA-TATE, followed by a similar VOI-based biodistribution analysis and identical human dosimetry estimation method using OLINDA software. The human dosimetry estimates from this analysis are shown in Table 5. These mouse-derived dosimetry estimates were then correlated with observed values from a recently published first-in-man study, as shown in Fig. 2. Some organs/tissue were predicted with very high precision (muscle, lung, red marrow, urinary bladder wall) whereas others were either over-estimated (osteogenic cells, heart wall) or under-estimated (liver, kidney, adrenals, spleen, pancreas) when comparing mouse-derived human dosimetry estimates and actual observed human dosimetry data. Importantly, the effective whole body dose was predicted with high precision (predicted value: 0.0252 mSv/Mbq, observed value: 0.0315 mSv/MBq) as shown in Fig. 2, thus validating our approach for human dosimetry estimation of ^{64}Cu-DOTA-AE105.

4. Discussion

This study provides the first human radiation dose estimates for ^{64}Cu-DOTA-AE105. The heart-wall, liver, osteogenic cells and small intestine are predicted to receive the highest absorbed dose. A total effective whole-body dose of 0.0317 mSv/MBq (female) and 0.0251 mSv/MBq (male) is predicted, thus resulting in an effective dose of 6.34 mSv and 5.02 mSv respectively, after injection of 200 MBq ^{64}Cu-DOTA-AE105. This is similar to radiation dose from a standard ^{18} F-FDG PET, where studies have found an absorbed dose of approximately 0.019 mSv/MBq, equal to an effective dose of 6.65 mSv after injection of 350 MBq [31,32] and more than 7 times below the 50 mSv dose limit used by the FDA for radiotracer human-study protocols [33]. A predictive effective dose of 0.0251 mSv/MBq is moreover also in the same range as different clinical used DOTA-conjugated peptides. ^{68}Ga-DOTANOC, ^{68}Ga-

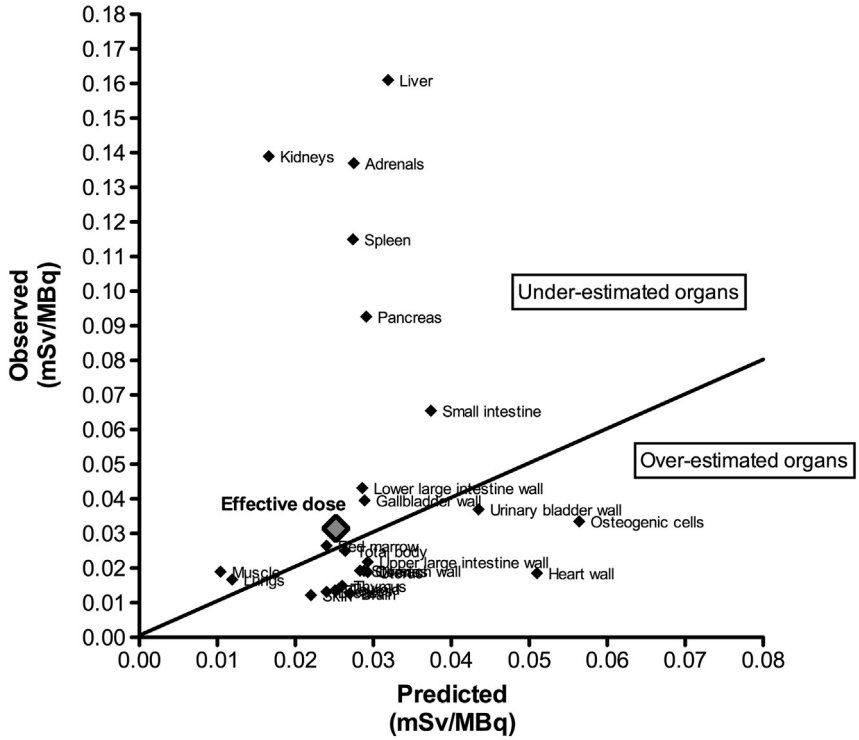

Fig. 2. Comparison between predicted and observed dose estimates and total effective dose (■) for ^{64}Cu-DOTA-TATE in humans. Mouse data based on three different time points. For further details please see text. Black line indicates optimal fit.

DOTATOC and ^{68}Ga-DOTATATE have been found to have an effective dose of 0.0167, 0.023 and 0.0257 mSv/MBq, respectively in humans [34–36].

Accordingly, from a dosimetry point of view, a clinical use of ^{64}Cu-DOTA-AE105 is feasible. Based on our validation data analysis using ^{64}Cu-DOTA-TATE as a model-compound, high precision in the total effective dose estimate was observed (predicted value: 0.025 mSv/MBq, observed value: 0.0315 mSv/MBq), thus validating the overall approach of using biodistibution data from image-derived three time-point nalysis, at least for ^{64}Cu-DOTA peptides. The ability to estimate single organ/tissue dosimetry, our analysis revealed a less clear picture. A group of organs was predicted with high precision such as muscle, lung and urinary bladder wall. Other organs where either under-estimated (liver, kidney) whereas others were over-estimated (osteogenic cells, heart wall). Similar observations have been reported earlier using this approach [22].

The discrepancy between mouse-derived dose estimates and human observed doses, most widely reflects the difference in metabolic rate between the two species. Furthermore, for an accurate dosimetry calculation, an adequate number of data points (measurements) and animal per time point should be used. Furthermore, the timing of these points must be carefully selected, since these points influence the confidence in the fit-to-data process for determining of the residence times. In this study we have used 5 animals per tracer, analyzed at three time-points. This are in agreement with other studies were the number of animals per time point typically are between 3–6, with the number of time points between 3 and 7 [20,21,26,27]. Despite the relatively low number of data points in this study (1, 4.5 and 22 h) it seems that three data points are sufficient considering the relatively high concordance between predicted and observed total body dosimetry values for ^{64}Cu-DOTA-TATE (Fig. 2 + Table 5). By analyzing the ratio (observed value divided by predicted value), the total body estimate is only 5% from the observed value (total body ratio: 0.95) and thus would not be significantly different from the predicted value. If this is a general phenomena or only valid for ^{64}Cu-DOTA-TATE, remains to be proven.

The high specific activity of our clinical batch protocol of ^{64}Cu-DOTA-AE105 only corresponds to a planned total injected dose of 1.5 μg (0.021 μg/kg body weight) compound when using 200 MBq activity/dose. Mice have previously been dosed with AE105 analogues at 60 mg/kg, with no toxicity observed [37] thus resulting in a safety margin of approximately 2.800.000 based on dose per body weight when dosing at 200 MBq/1.5 μg. Moreover, our PET studies in mice have also revealed no acute toxicity when dosing ^{64}Cu-DOTA-AE105 at 8 mg/kg. Finally, peptide-based PET imaging using ^{64}Cu-DOTA seem well tolerated since no toxicity has been reported in more than 200 patients PET scanned with ^{64}Cu-DOTA-TATE (unpublished data).

In conclusion, the favorable dosimetry estimates together with previously reported uPAR PET data fully support future human testing of ^{64}Cu-DOTA-AE105.

References

[1] Dano K, Behrendt N, Hoyer-Hansen G, Johnsen M, Lund LR, Ploug M, et al. Plasminogen activation and cancer. Thromb Haemost 2005;93:676–81.
[2] Blasi F, Sidenius N. The urokinase receptor: focused cell surface proteolysis, cell adhesion and signaling. FEBS Lett 2010;584:1923–30.
[3] Jacobsen B, Ploug M. The urokinase receptor and its structural homologue C4.4A in human cancer: expression, prognosis and pharmacological inhibition. Curr Med Chem 2008;15:2559–73.
[4] Rasch MG, Lund IK, Almasi CE, Hoyer-Hansen G. Intact and cleaved uPAR forms: diagnostic and prognostic value in cancer. Front Biosci 2008;13:6752–62.
[5] Ganesh S, Sier CF, Heerding MM, Griffioen G, Lamers CB, Verspaget HW. Urokinase receptor and colorectal cancer survival. Lancet 1994;344:401–2.
[6] Rabbani SA, Xing RH. Role of urokinase (uPA) and its receptor (uPAR) in invasion and metastasis of hormone-dependent malignancies. Int J Oncol 1998;12:911–20.
[7] Riisbro R, Christensen IJ, Piironen T, Greenall M, Larsen B, Stephens RW, et al. Prognostic significance of soluble urokinase plasminogen activator receptor in serum and cytosol of tumor tissue from patients with primary breast cancer. Clin Cancer Res 2002;8:1132–41.
[8] Piironen T, Haese A, Huland H, Steuber T, Christensen IJ, Brunner N, et al. Enhanced discrimination of benign from malignant prostatic disease by selective measurements of cleaved forms of urokinase receptor in serum. Clin Chem 2006;52:838–44.
[9] Lomholt AF, Christensen IJ, Hoyer-Hansen G, Nielsen HJ. Prognostic value of intact and cleaved forms of the urokinase plasminogen activator receptor in a retrospective study of 518 colorectal cancer patients. Acta Oncol 2010;49:805–11.
[10] Almasi CE, Brasso K, Iversen P, Pappot H, Hoyer-Hansen G, Dano K, et al. Prognostic and predictive value of intact and cleaved forms of the urokinase plasminogen activator receptor in metastatic prostate cancer. Prostate 2011;71:899–907.
[11] Alpizar-Alpizar W, Christensen IJ, Santoni-Rugiu E, Skarstein A, Ovrebo K, Illemann M, et al. Urokinase plasminogen activator receptor on invasive cancer cells: a prognostic factor in distal gastric adenocarcinoma. Int J Cancer 2012;131:E329–36.
[12] Boonstra MC, Verspaget HW, Ganesh S, Kubben FJ, Vahrmeijer AL, van de Velde CJ, et al. Clinical applications of the urokinase receptor (uPAR) for cancer patients. Curr Pharm Des 2011;17:1890–910.
[13] Persson M, Kjaer A. Urokinase-type plasminogen activator receptor (uPAR) as a promising new imaging target: potential clinical applications. Clin Physiol Funct Imaging 2013;33(5):329–37.
[14] Yang Y, Adelstein SJ, Kassis AI. General approach to identifying potential targets for cancer imaging by integrated bioinformatics analysis of publicly available genomic profiles. Mol Imaging 2011;10:123–34.
[15] Kriegbaum MC, Persson M, Haldager L, Alpizar-Alpizar W, Jacobsen B, Gardsvoll H, et al. Rational targeting of the urokinase receptor (uPAR): development of antagonists and non-invasive imaging probes. Curr Drug Targets 2011;12:1711–28.
[16] Persson M, Madsen J, Ostergaard S, Jensen MM, Jorgensen JT, Juhl K, et al. Quantitative PET of human urokinase-type plasminogen activator receptor with 64Cu-DOTA-AE105: implications for visualizing cancer invasion. J Nucl Med 2012;53:138–45.
[17] Persson M, Madsen J, Ostergaard S, Ploug M, Kjaer A. (68)Ga-labeling and in vivo evaluation of a uPAR binding DOTA- and NODAGA-conjugated peptide for PET imaging of invasive cancers. Nucl Med Biol 2012;39:560–9.
[18] Persson M, Liu H, Madsen J, Cheng Z, Kjaer A. First F-labeled ligand for PET imaging of uPAR: In vivo studies in human prostate cancer xenografts. Nucl Med Biol 2013;40(5):618–24.
[19] Persson M, HM, Madsen J, Jørgensen TJD, Jensen KJ, Kjaer A, et al. Improved PET imaging of uPAR expression using new 64Cu-labeled cross-bridged peptide ligands: comparative in vitro and in vivo studies. Theranostics 2013;3:618–32.
[20] Lesche R, Kettschau G, Gromov AV, Bohnke N, Borkowski S, Monning U, et al. Preclinical evaluation of BAY 1075553, a novel F-labelled inhibitor of prostate-specific membrane antigen for PET imaging of prostate cancer. Eur J Nucl Med Mol Imaging 2013;41(1):89–101.
[21] Xavier C, Vaneycken I, D'Huyvetter M, Heemskerk J, Keyaerts M, Vincke C, et al. Synthesis, preclinical validation, dosimetry, and toxicity of 68Ga-NOTA-anti-HER2 Nanobodies for iPET imaging of HER2 receptor expression in cancer. J Nucl Med 2013;54:776–84.
[22] Sakata M, Oda K, Toyohara J, Ishii K, Nariai T, Ishiwata K. Direct comparison of radiation dosimetry of six PET tracers using human whole-body imaging and murine biodistribution studies. Ann Nucl Med 2013;27:285–96.
[23] Santens P, De Vos F, Thierens H, Decoo D, Slegers G, Dierckx RA, et al. Biodistribution and dosimetry of carbon-11-methoxyprogabidic acid, a possible ligand for GABA-receptors in the brain. J Nucl Med 1998;39:307–10.
[24] Bencherif B, Endres CJ, Musachio JL, Villalobos A, Hilton J, Scheffel U, et al. PET imaging of brain acetylcholinesterase using [11C]CP-126,998, a brain selective enzyme inhibitor. Synapse 2002;45:1–9.
[25] Sakata M, Wu J, Toyohara J, Oda K, Ishikawa M, Ishii K, et al. Biodistribution and radiation dosimetry of the alpha7 nicotinic acetylcholine receptor ligand [11C]CHIBA-1001 in humans. Nucl Med Biol 2011;38:443–8.
[26] Lee CL, Wahnishe H, Sayre GA, Cho HM, Kim HJ, Hernandez-Pampaloni M, et al. Radiation dose estimation using preclinical imaging with 124I-metaiodobenzylguanidine (MIBG) PET. Med Phys 2010;37:4861–7.
[27] Bretin F, Warnock G, Bahri MA, Aerts J, Mestdagh N, Buchanan T, et al. Preclinical radiation dosimetry for the novel SV2A radiotracer [18 F]UCB-H. EJNMMI Res 2013;3:35.
[28] Pfeifer A, Knigge U, Mortensen J, Oturai P, Berthelsen AK, Loft A, et al. Clinical PET of neuroendocrine tumors using 64Cu-DOTATATE: first-in-humans study. J Nucl Med 2012;53:1207–15.
[29] Kirschner AS, Ice RD, Beierwaltes WH. Radiation dosimetry of 131I-19-iodocholesterol. J Nucl Med 1973;14:713–7.
[30] Stabin MG, Siegel JA. Physical models and dose factors for use in internal dose assessment. Health Phys 2003;85:294–310.
[31] Deloar HM, Fujiwara T, Shidahara M, Nakamura T, Watabe H, Narita Y, et al. Estimation of absorbed dose for 2-[F-18]fluoro-2-deoxy-D-glucose using whole-body positron emission tomography and magnetic resonance imaging. Eur J Nucl Med 1998;25:565–74.
[32] Deloar HM, Fujiwara T, Shidahara M, Nakamura T, Yamadera A, Itoh M. Internal absorbed dose estimation by a TLD method for 18 F-FDG and comparison with the dose estimates from whole body PET. Phys Med Biol 1999;44:595–606.
[33] Administration USFaD. 21 CFR Part 361. Prescription drugs for human use generally recognized as safe and effective and not misbranded: drugs used in, research; 2009.

[34] Pettinato C, Sarnelli A, Di Donna M, Civollani S, Nanni C, Montini G, et al. 68Ga-DOTANOC: biodistribution and dosimetry in patients affected by neuroendocrine tumors. Eur J Nucl Med Mol Imaging 2008;35:72–9.
[35] Hartmann H, Zophel K, Freudenberg R, Oehme L, Andreeff M, Wunderlich G, et al. Radiation exposure of patients during 68Ga-DOTATOC PET/CT examinations. Nuklearmedizin (Nuclear medicine) 2009;48:201–7.
[36] Walker RC, Smith GT, Liu E, Moore B, Clanton J, Stabin M. Measured human dosimetry of 68Ga-DOTATATE. J Nucl Med 2013;54:855–60.
[37] Ploug MØ, S. Holst-Hansen, C. Stephens, R. Dano, K. Holm, A. Peptide antagonists of the human urokinase receptor and method for selecting them. In: US Patent editor. United States of America: Cancerforskningsfonden AF 1989; 2006, p. 34.